HELICOPTER INVERSE SIMULATION INCORPORATING AN INDIVIDUAL BLADE ROTOR MODEL

Stephen Rutherford
Postgraduate Researcher

Dr Douglas G. Thomson
Lecturer in Flight Dynamics

Department of Aerospace Engineering
University of Glasgow
Glasgow, U.K.

Abstract

Inverse simulation is used to calculate the control displacements required for a modelled vehicle to perform a particular manoeuvre. As with all simulations the usefulness of the technique depends on the validity of the mathematical model used. To incorporate the latest forms of helicopter model ("individual blade models") in an inverse framework, it has been necessary to modify existing inverse techniques. Such a model is described in this paper along with an inverse algorithm capable of accommodating it. The resulting simulation is validated against flight data and comparisons are made with a more basic model.

Nomenclature

a	speed of sound in air
$a_{x\,hinge}^{shaft}$, $a_{z\,hinge}^{shaft}$	translational acceleration components of hinge referred to shaft axes
$c_{elem.}$	elemental chord
C_l, C_d	local elemental lift and drag coefficients
h	height of obstacle in pop-up manoeuvre
I_β, M_β	blade flapping inertia and mass moment
$[J]$	Jacobian matrix
K_β	blade hinge spring stiffness
$\bar{l}_{elem.}$, $\bar{d}_{elem.}$	elemental lift and drag per unit span
l_{hub}, h_{hub}	distances from the fuselage reference point to the main rotor hub centre
M	local Mach number
$M_{aero.}$	aerodynamic moment acting at blade hinge
P, Q, R	helicopter angular velocity components
r, $r_{elem.}$	spanwise distance to blade element centre from hub and hinge respectively
R	rotor radius
$\underline{r}$	position vector
s	distance to obstacle in pop-up
t	time
t_m	time taken to complete pop-up manoeuvre
$[T]$	transformation matrix
U, V, W	translational velocity components of helicopter centre of gravity
$\underline{u}$	control vector
$\underline{u}_{error}$	control error vector
$v_{aero.}$	aerodynamic velocity
$v_{ind.}$	induced velocity
$v_{tan.}$, $v_{perp.}$	tangential and perpendicular velocity components of air
$\underline{v}$	translational velocity vector
V_f	helicopter flight velocity
x_e, y_e, z_e	displacements relative to an earth fixed inertial frame
$x_{ref.}$, $z_{ref.}$	distances from the helicopter centre of gravity to the fuselage reference point
$\underline{x}$	state vector
$\underline{y}$	output vector
$\underline{y}_{desired}$, $\underline{y}_{error}$	desired and error output vectors
α	blade element angle of attack
α_y^{shaft}	shaft axes angular acceleration
$\underline{\alpha}$	rotational acceleration vector
β	blade flap angle
Δt	manoeuvre discretisation interval
ϕ	blade element inflow angle
ϕ, θ, ψ	aircraft attitude angles
$\gamma_{sh.}$	shaft tilt angle
θ	blade element pitch angle
θ_0	main rotor collective pitch angle
θ_{1s}, θ_{1c}	longitudinal and lateral cyclic pitch angles
θ_{0tr}	tail rotor collective pitch angle
θ_{twist}	blade geometric twist
ρ	local air density
$\underline{\omega}$	rotational velocity vector
ψ	blade azimuthal position

1. Introduction: Rotorcraft Modelling and Inverse Simulation

The conventional approach adopted in flight simulation is to calculate the response of a modelled vehicle to prescribed control inputs. This is achieved by integrating the differential equations of motion, allowing the vehicle's trajectory to be computed in response to a defined pilot control sequence. Interest in an alternative approach known as "inverse simulation" is growing. As might be deduced, this form of simulation involves calculating the pilot inputs required for a modelled vehicle to fly a prescribed trajectory or manoeuvre. Inverse simulation is particularly useful in studies of flight involving precision manoeuvring. At the University of Glasgow applications have been related to helicopter flight dynamics and have included studies of safety during take-off from off-shore platforms[1], manoeuvrability in nap-of-the-earth flight[2] and workload whilst flying ADS-33 Mission Task Elements[3]. Other researchers have applied this technique to control systems studies[4] and helicopter agility[5].

The helicopter inverse simulation developed at Glasgow, "Helinv"[6], makes use of a mathematical model known as "HGS"[7] (Helicopter Generic Simulation) which describes a single main and tail rotor helicopter. This is a nonlinear model with 7 degrees of freedom (the usual 6 body modes plus rotorspeed) and has what is termed a "disc" representation of the main and tail rotors. In this form of rotor model, elemental blade forces are calculated from simplified linear aerodynamic relationships and expressed as functions of azimuthal and radial position. The elemental forces are then integrated symbolically to give closed loop expressions for the rotor forces and moments. Clearly this type of model is limited as it is not possible to accommodate nonlinear aerodynamic properties such as Mach number variation, 3-D blade tip effects or retreating blade stall - all of which have significant influence on the thrust generated by the rotor. Nonetheless this model has provided useful and valid results[8] for a wide range of applications.

To further extend the range of applicability (allowing valid simulation at the extremes of the flight envelope) requires the development of a more comprehensive model. The natural progression is to a so called "individual blade" model where the disc representation of the rotor is replaced by individual models of each of its blades. Elemental blade forces are integrated numerically allowing more accurate representation of the aerodynamic properties to be included. Another fundamental difference between the two models is that the rotor loads calculated by the disc model are in effect averaged for a complete revolution of all of the blades i.e. a single steady value is computed over the period of rotation. This is in contrast to the individual blade model where the effect on the blade loads due to the periodicity of their motion (caused by the cyclic application of blade pitch) is fully captured. Consequently the rotor forces calculated (which are subsequently applied to the body equations) are periodic. Such a model, known as "Hibrom"[9] (Helicopter Individual Blade Rotor Model) has been developed at Glasgow, details of which are presented in Section 3 of this paper.

The numerical techniques associated with inverse simulation are still to a large extent under development[10, 11, 12]. The methods currently used fall into two categories: those employing numerical differentiation; and those using numerical integration to solve the equations of motion. Using the numerical differentiation approach the problem is discretised as all of the state variable rates are effectively calculated by numerical differencing. The differential equations of motion become algebraic and are readily solved for the control inputs. The alternative method uses repeated numerical integration of the equations of motion to determine the control displacements required to move the aircraft between closely spaced positional co-ordinates.

Helinv is an example of a differentiation based inverse simulation. As discussed above there is a need to replace the disc model (HGS) originally implemented in Helinv with a more comprehensive individual blade model (Hibrom). Unfortunately such a model does not lend itself well to implementation in an inverse form, at least as far as the numerical differentiation method is concerned. This is partly due to the structure of the model but mainly due to the range of characteristic frequencies associated with the dynamics of the helicopter. Selection of an appropriate value for the time interval for the numerical differentiation becomes a difficult problem. The disc model only captures the low frequency body modes of the aircraft, so a relatively large time step can be used for differencing (possibly as large as 0.1s) and hence rounding errors are usually avoided. This is not the case for the individual blade model where the higher frequency rotor dynamics require a much smaller time interval to evaluate their rates (typically less than 0.01s). Experience has shown that this will lead to rounding error problems in the much more slowly moving body modes (for example in a side-step manoeuvre the fuselage pitch attitude will change very little over a 0.01s interval and hence the calculation of its rate may be prone to rounding error). Experience has also shown that these rounding errors eventually lead to failure of the inverse algorithm itself.

In order to implement an individual blade rotor model in an inverse sense, the alternative approach offered by the numerical integration technique is required. Unfortunately this method can also exhibit unwanted features[11, 12]. Work at Glasgow has solved many of the difficulties associated with this simulation technique[10] and a generic inverse simulation known as "Genisa" (Generic Inverse Simulation Algorithm) has been devised. The resulting methodology is presented in Section 2 along with a summary of the advances made during its development.

A crucial element of any simulation exercise is the validation of results. Section 4 of this paper presents comparisons between an inverse simulation of a "quick-

hop" manoeuvre and the actual manoeuvre flown by a Lynx helicopter. Further, a comparison of inverse simulation results between the two rotor models (individual blade and disc) shows the advantages to be gained in using an individual blade rotor model in terms of the significant rotor information which is derived.

2. Development of a Robust and Stable Generic Inverse Simulation Methodology

In all cases the initial phase of any inverse simulation is the definition of the trajectory or manoeuvre which is to be flown. This acts as the input to the simulation, and a typical example of one such manoeuvre definition is now presented.

2.1 The Manoeuvre Definition

Manoeuvres are defined essentially as a series of positional co-ordinates (relative to an earth fixed frame of reference), equally spaced in time ($x_e(t)$, $y_e(t)$, $z_e(t)$). The helicopter's component velocities ($\dot{x}_e(t)$, $\dot{y}_e(t)$, $\dot{z}_e(t)$) and accelerations ($\ddot{x}_e(t)$, $\ddot{y}_e(t)$, $\ddot{z}_e(t)$) in the earth fixed frame of reference are then obtained by differentiation. Though this ensures that the vehicle's centre of gravity follows the correct trajectory, it is still free to adopt an unspecified attitude. It is therefore necessary to prescribe one of the vehicle attitude angles (the heading angle, $\psi(t)$ being the most convenient) to guarantee a realistic manoeuvre and vehicle response. Thus the desired output vector, $\underline{y}_{desired}$ can be easily constructed using three earth fixed displacements and heading:

$$\underline{y}_{desired} = [x_e \quad y_e \quad z_e \quad \psi]^T \tag{1}$$

and is, in effect, the input to the inverse simulation.

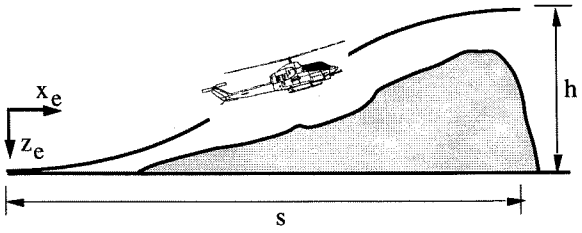

Figure 1: The Pop-up Manoeuvre

As an example consider the "pop-up", Figure 1, where it is assumed that the pilot's task is to clear an obstacle, height h over some distance, s. The obstacle is assumed to be located at the end of the manoeuvre. A series of boundary conditions are applied to the altitude of the helicopter at the entry and exit of the manoeuvre. The simplest analytical function which satisfies these conditions is fifth order polynomial:

$$z_e(t) = -h\left[6\left(\frac{t}{t_m}\right)^5 - 15\left(\frac{t}{t_m}\right)^4 + 10\left(\frac{t}{t_m}\right)^3\right] \tag{2}$$

where t_m is the time taken to complete the manoeuvre. To complete the description we assume that the pop-up is performed at constant heading (i.e. $\psi(t) = 0$) and velocity, V_f, and that there are no lateral excursions (i.e. the manoeuvre is longitudinal and performed in the $x_e - z_e$ plane, $y_e(t) = 0$). The longitudinal displacement $x_e(t)$ can be evaluated numerically by integrating:

$$\dot{x}_e(t) = \sqrt{V_f^2 - \dot{z}_e(t)^2}$$

whilst the manoeuvre time, t_m, can be calculated by specifying the total track distance s, then noting that:

$$s = \int_0^{t_m} \dot{x}_e(t)dt.$$

In essence the complete manoeuvre may be defined by specifying values for the parameters s, h and V_f. This approach may seem simplistic but past experience[2] has shown that profiles such as that given in equation (2) provide realistic trajectories.

This manoeuvre definition must now be applied to the helicopter model in such a way that the control displacements necessary to fly it are calculated. The scheme used by Rutherford and Thomson is presented in detail in Reference 10, and for clarity this is now summarised.

2.2 The Genisa Algorithm

The nonlinear equations of motion may be expressed in the form:

$$\dot{\underline{x}} = \underline{f}(\underline{x}, \underline{u}); \quad \underline{x}(0) = \underline{x}_0,$$

$$\underline{y} = \underline{g}(\underline{x})$$

where $\underline{u}$ is the control vector, $\underline{x}$ the state vector, and $\underline{y}$ the output vector. For the helicopter we have:

$$\underline{x} = [U \quad V \quad W \quad P \quad Q \quad R \quad \phi \quad \theta \quad \psi]^T$$

and

$$\underline{u} = [\theta_0 \quad \theta_{1_s} \quad \theta_{1_c} \quad \theta_{0_{tr}}]^T$$

where θ_0 is the main rotor collective pitch angle, θ_{1s} the longitudinal cyclic, θ_{1c} the lateral cyclic and θ_{0tr} the tail rotor collective pitch angle. The output vector, $\underline{y}$, is given by equation (1). In the context of an inverse simulation we require to calculate $\underline{u}$ for a given $\underline{y}$. The

problem can be discretised into a series of time points t_k at each of which there is a desired output vector $\underline{y}_{desired}(t_k)$ (as defined by the manoeuvre model) describing the position and heading of the helicopter. At the current time point $t = t_k$, the value of $\underline{x}(t_k)$ is known by integration of the state derivatives, $\dot{\underline{x}}(t_{k-1})$, from the previous time point $t = t_{k-1}$. The influence of the control vector, $\underline{u}(t_k)$ on $\dot{\underline{x}}(t_k)$ (and consequently $\underline{x}(t_{k+1})$ and $\underline{y}(t_{k+1})$) can be found by perturbing the current value. The problem is effectively to find a solution for the control vector $\underline{u}(t_k)$ which will produce a value of $\underline{y}(t_{k+1})$ equal to $\underline{y}_{desired}(t_{k+1})$. In simple terms a guess is made as to what control inputs are required to move the helicopter from its current position (and heading) to that specified at the next time point in the manoeuvre definition. The equations of motion are then integrated in the usual manner and the actual position produced using the estimated control displacements is calculated. The error between actual and desired position is then used as the basis for an iterative scheme to calculate exactly what control displacements are required to achieve the desired positional and heading change. The output error functions are solved over each interval, producing control time histories for the complete manoeuvre. This method has been used previously, by Gao and Hess[12] amongst others.

At a general time point (the m^{th} estimate at the k^{th} time point) $\dot{\underline{x}}(t_k)_m$ can be evaluated using $\underline{x}(t_k)$ and the current estimate for $\underline{u}(t_k)_m$:

$$\dot{\underline{x}}(t_k)_m = \underline{f}\left[\underline{x}(t_k), \underline{u}(t_k)_m\right]. \tag{3}$$

This in turn can be integrated, using for example the method of Runge-Kutta[13], to produce estimates of $\underline{x}(t_{k+1})_m$ and $\underline{y}(t_{k+1})_m$ at the next time point:

$$\underline{x}(t_{k+1})_m = \int_{t_k}^{t_{k+1}} \dot{\underline{x}}(t_k)_m dt + \underline{x}(t_k)_m, \tag{4}$$

$$\underline{y}(t_{k+1})_m = \underline{g}\left[\underline{x}(t_{k+1})_m\right]. \tag{5}$$

An error function is defined as the difference between the latest estimate of the output vector, $\underline{y}(t_{k+1})_m$ and the desired value $\underline{y}_{desired}(t_{k+1})$:

$$\underline{y}_{error}(t_{k+1})_m = \underline{y}(t_{k+1})_m - \underline{y}_{desired}(t_{k+1}). \tag{6}$$

The conventional approach[12] is to seek the condition $\underline{y}_{error}(t_{k+1})_m = \underline{0}$, usually by employing a Newton-Raphson solver such as:

$$\underline{u}(t_k)_{m+1} = \underline{u}(t_k)_m - [J]^{-1}\underline{y}_{error}(t_{k+1})_m, \tag{7}$$

where the Jacobian, $[J]$ describes the rate of change of the output vector with respect to the control vector. The details of the Jacobian formulation are given in the next section. Genisa uses a modified form of this iteration,

$$\underline{u}(t_k)_{m+1} = \underline{u}(t_k)_m - \underline{u}_{error}(t_k)_m,$$

which in contrast to equation (7) does not involve inverting the Jacobian explicitly. Instead the control error vector is evaluated by solution of the linear system in equation (8) using LU Factorisation[13]:

$$[J]\underline{u}_{error}(t_k)_m = \underline{y}_{error}(t_{k+1})_m. \tag{8}$$

This method, by avoiding matrix inversion, should be more accurate and stable for a wider range of Jacobians.

2.2.1 Evaluation of the Jacobian

Assuming that the problem to be solved involves a vehicle with n controls flying a manoeuvre defined by n parameters then for the m^{th} estimate at the k^{th} time point, the Jacobian is an $n \times n$ matrix, the entries of which, $j_{ij}(t_k)_m$ are evaluated by differentiating each of the elements of the output error vector $y_{error\,i}(t_{k+1})_m$ with respect to each of the elements of the control vector $u_j(t_k)_m$. The expression for determining a Jacobian element is thus:

$$j_{ij}(t_k)_m = \frac{\partial y_{error\,i}(t_{k+1})_m}{\partial u_j(t_k)_m}.$$

If the desired output is defined in terms of displacements then the Jacobian is:

$$[J] = \begin{bmatrix} \frac{\partial x_e}{\partial \theta_0} & \frac{\partial x_e}{\partial \theta_{1s}} & \frac{\partial x_e}{\partial \theta_{1c}} & \frac{\partial x_e}{\partial \theta_{0tr}} \\ \frac{\partial y_e}{\partial \theta_0} & \bullet & \bullet & \bullet \\ \frac{\partial z_e}{\partial \theta_0} & \bullet & \bullet & \bullet \\ \frac{\partial \psi}{\partial \theta_0} & \bullet & \bullet & \frac{\partial \psi}{\partial \theta_{0tr}} \end{bmatrix},$$

where the variables are as defined earlier. Within the algorithm, there are no analytical expressions for the output vector, $\underline{y}$ and so the elements of the Jacobian must be calculated numerically by central differencing, the general representation of which is given below:

$$\frac{\partial y_{error\,i}(t_{k+1})_m}{\partial u_j(t_k)_m} = \left[y_{error\,i}\left(t_{k+1}, \left(u_j(t_k) + \delta u_j(t_k)\right)\right)_m - y_{error\,i}\left(t_{k+1}, \left(u_j(t_k) - \delta u_j(t_k)\right)\right)_m \right] / 2\delta u_j(t_k)_m$$

All n output elements must be calculated at positive and negative perturbations from their current estimates and hence equations (3-6) must be used a further $2n$ times. This process is repeated at a series of consecutive, equally spaced points in time along the manoeuvre giving time histories for the controls.

2.3 Structural Differences Between Integration and Differentiation Methods

The most significant difference between the two types of solution is the time taken to produce results: Genisa is typically an order of magnitude slower then Helinv, mainly due to the large number of numerical integrations which have to be performed. Though this is a major drawback of the integration approach, its main advantage lies in the algorithm structure. In the differentiation method the necessity to express the rates of change of state variables by numerical differentiation forces the vehicle equations of motion to become embedded within the main inverse algorithm. As a result, making major changes to the model (or indeed to the form of the output $\underline{y}_{desired}$) can require significant restructuring of the algorithm. This is not the case in methods using the integration scheme where the model and algorithm can be expressed independently. This is primarily because the iteration minimises the error in flight path variables which are not explicit in the equations of motion. The result of this is that modelling enhancements do not necessitate changes in the algorithm structure; indeed it is possible to simulate completely different vehicles simply by changing the mathematical model. Further, should an alternative set of input motion constraints be desirable then it is a simple case to modify the error functions. It is for these reasons, and espite the greatly increased computational time required, that the integration based method is often favoured.

2.4 Improving the Numerical Stability of Integration Based Inverse Simulations

The stability of solutions generated using the integration method can be compromised if too small a calculation time step, Δt is used. As first noted by Lin et al[11]: *"when there is an uncontrolled state variable, the integration inverse method may be unstable for small time step"*. This can be demonstrated by considering inverse simulation using the HGS model with multiblade flapping dynamics. As a conventional helicopter has only four controls and the model in question has 10 degrees of freedom it is clear that there will be uncontrolled states. The Genisa simulation does show evidence of the phenomenon identified by Lin; the pop-up results in Figure 2 (where s = 250m, h = 30m, V_f = 80 knots) for example were produced using a time step of 0.01 seconds. The small discretisation interval has introduced unstable oscillations whose period matches the size of Δt. This result is typical of those observed in other inverse simulations of this type and is without doubt a serious drawback to the use of such techniques. In the case of systems which have a wide range of characteristic frequencies, such as the helicopter, these problems can be restrictive. Indeed for a more sophisticated individual

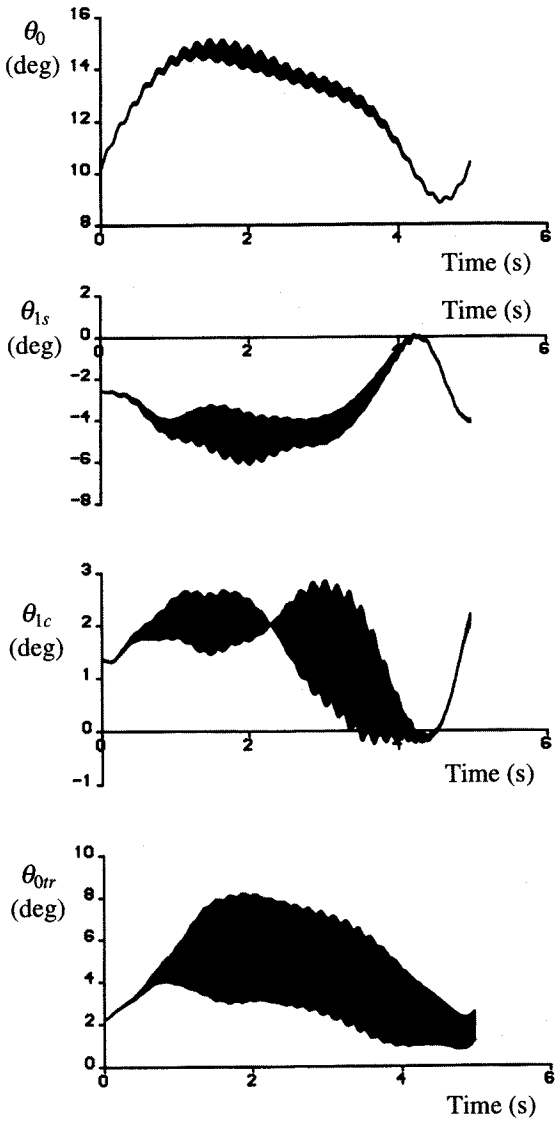

Figure 2: Inverse Simulation Results Using Displacement Error Function (HGS Model, Westland Lynx Flying Pop-up)

blade, helicopter model to be utilised for inverse simulation, a solution to the problem of numerical stability with small time steps is essential.

It is shown in Section 2.2, equation (6), that the iterative solution most often used in integration inverse algorithms is based upon minimising the difference between the actual and desired helicopter position:

$$\underline{y} - \underline{y}_{desired} = \underline{0} \tag{9}$$

where the output vector $\underline{y}$ contains the elements x_e, y_e, z_e and ψ. The rationale behind making this choice is

that it is most convenient and natural to describe a manoeuvre in terms of these parameters. A simple alternative to this is that the error to be minimised is defined in terms of the aircraft's acceleration i.e. the output vector $\underline{y}$ contains the elements $\ddot{x}_e$, $\ddot{y}_e$, $\ddot{z}_e$ and $\ddot{\psi}$. In the manoeuvre definition used to initiate the simulation the desired accelerations are evaluated simply by differentiating the representative polynomials (equation (2) for example is readily differentiated to give $\ddot{z}_e$ etc.). The algorithm as described in Section 2.2 is unchanged; that is, estimates of control displacements are made and the equations of motion are integrated between time points until equation (9) is satisfied.

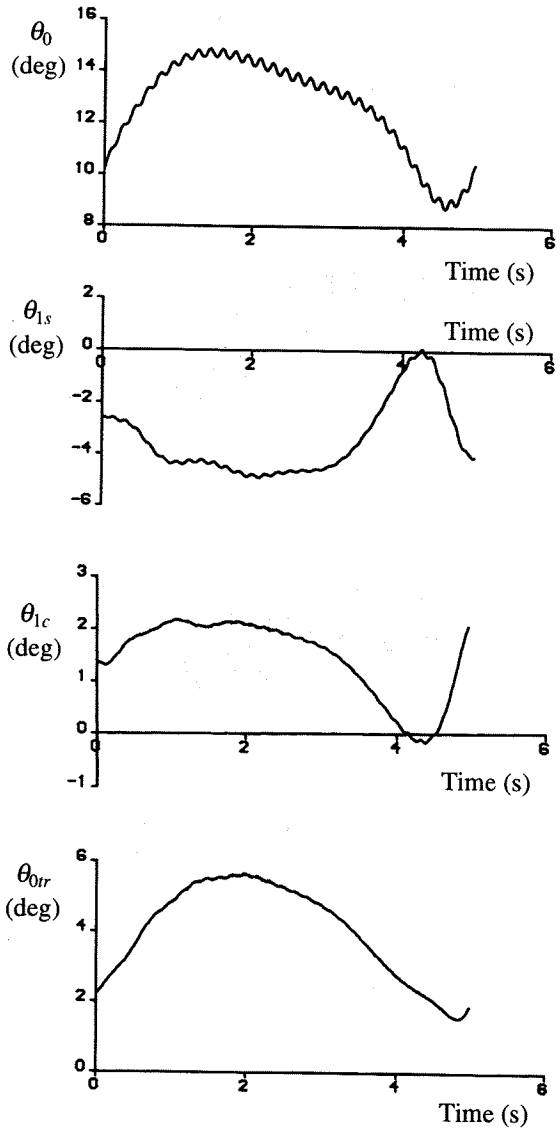

Figure 3: Inverse Simulation Results Using Acceleration Error Function (HGS Model, Westland Lynx Flying Pop-up)

This simple modification has the effect of eliminating the instabilities observed previously. Figure 3 shows controls calculated for the sample pop-up described earlier, again using a time step of 0.01 seconds. Direct comparison can then be made between Figures 2 and 3 and it is evident that the instabilities associated with a small time increment have been eliminated leaving only low amplitude oscillations associated with blade flapping. It is apparent then that a simple modification has produced a significant improvement in the quality of the results. A complete explanation of why such a dramatic improvement is achieved is given by Rutherford and Thomson[10]. In summary, however, the underlying reason is that an error function associated with accelerations will have greater sensitivity to control displacements than will one associated with positional displacements. This has implications when using numerical differentiation to calculate the Jacobian. When using a very short time interval the positional displacements due to small perturbations in controls may be similar and very small, hence leading to rounding errors in the differencing process. This may not be the case using the more sensitive acceleration error vector where even small positive and negative control displacements should provide distinct and differentiable function values.

It has been shown in this section that it is possible to obtain stable inverse simulation results using an inverse simulation technique the structure of which is capable of accommodating a complex (individual blade) rotorcraft model. This combination is demonstrated in section 4 of this paper, however it is first necessary to give some details of the individual blade helicopter mathematical model itself.

3. Development of an Individual Blade Rotorcraft Model, Hibrom

To successfully simulate the dynamics of a given aircraft requires calculation of the external forces and moments generated by each of the vehicle's components. For a helicopter, modelling the main rotor occupies the majority of effort as this is the most complex component. The forces and moments generated by a helicopter rotor are most conveniently estimated by use of Blade Element Theory[14]. As already discussed in the context of helicopter simulation, there are two commonly adopted approaches: the *Disc Model* and the *Individual Blade Model*. Blade element theory is used in both cases to calculate the rotor forces and moments. The primary difference between the two model types is that simplifying assumptions regarding the aerodynamic properties of the blade elements are made in the disc model to allow analytical expressions to be derived. As will now be shown, this is not the case in an individual blade model where, as the integrations are performed numerically, it is possible to incorporate a more comprehensive representation of the aerodynamic and geometrical properties of the blade. The main modelling features of Hibrom are now summarised, a more detailed description is given by Rutherford and Thomson[9].

3.1 Hibrom: Model Features

i) *Blade Dynamics*

It is assumed that the main and tail rotor blades are fully rigid. This assumption has been found to be reasonable for simulating the flight mechanics of articulated rotor configurations[15], but may result in poor prediction of the off-axis response of helicopters with semi-rigid rotors[16]. Lead/lag freedom has also been neglected.

ii) *Blade Aerodynamics*

Aerodynamic data is for a NACA 0012 aerofoil[14] in the range ±18° and compressibility effects have been included. The data has been blended with suitable low speed data for the remainder of the 360° range to model the reversed flow region and fully stalled retreating blades. Dynamic stall effects have not been included.

iii) *Inflow model.*

The dynamic inflow model of Peters and HaQuang[17] has been used. This model captures the effect of the rotor moments and the lag between application of the blade pitch and changes in the aerodynamic forces.

iv) *Blade geometry*

The spanwise variation of chord and geometric twist have been included in the blade elemental data.

v) *Fuselage Aerodynamics*

Look-up tables of force and moment coefficients generated from wind tunnel tests of fuselage models have been used. The full 360° range of angle of attack and sideslip are accommodated.

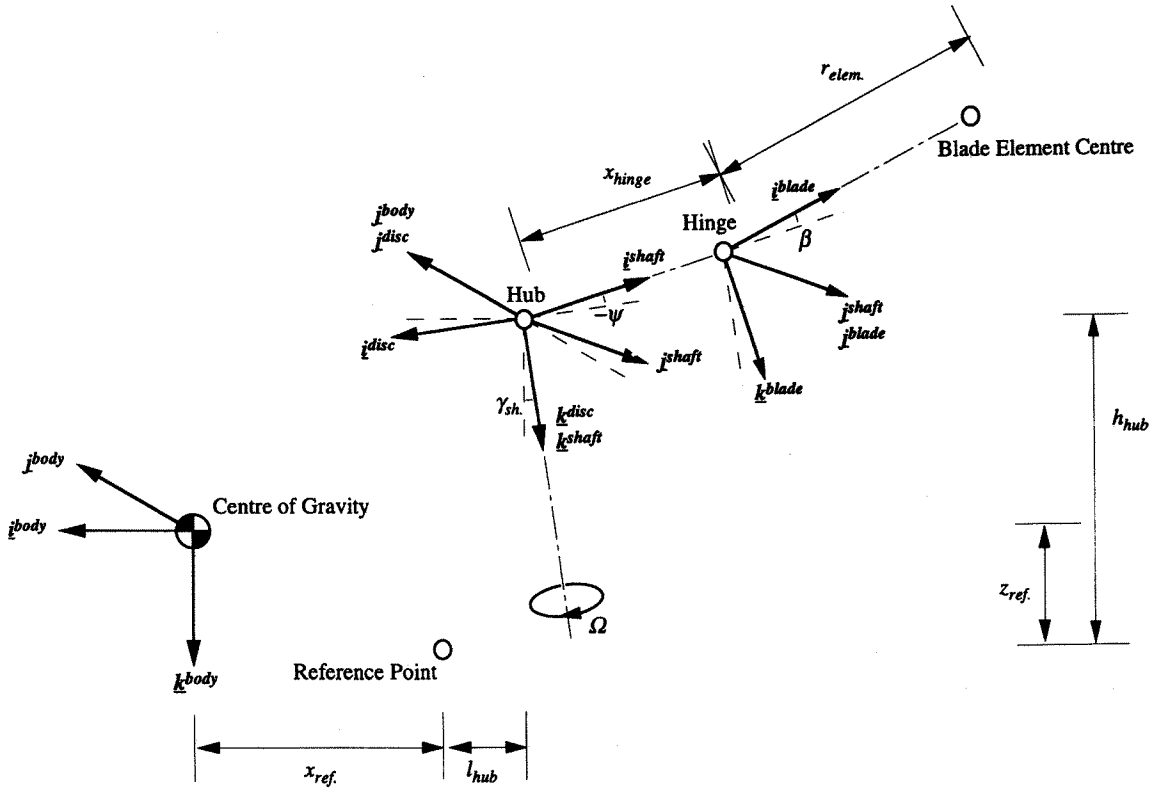

Figure 4: Axes Sets Required to Obtain Blade Element Velocity and Accelerations

3.2 Blade Element Kinematics

To calculate the forces acting upon each blade element it is necessary to first determine their respective velocities and accelerations. Figure 4 illustrates the axes transformations required to find the velocity and acceleration of a blade element, given that the kinematics of the helicopter centre of gravity are known. The system is assumed to be fully rigid. The first stage is to describe, in *body* axes, the velocity of the hub centre with respect to the helicopter's centre of gravity:

$$\underline{v}_{hub}^{body} = \underline{v}_{c.g.}^{body} + \underline{\omega}^{body} \times \underline{r}_{c.g./hub}^{body},$$

where $$\underline{v}_{c.g.}^{body} = \{U \quad V \quad W\}^T,$$

$$\underline{\omega}^{body} = \{P \quad Q \quad R\}^T,$$

and $\underline{r}_{c.g./hub}^{body} = \left\{ x_{ref.} + l_{hub} \quad 0 \quad z_{ref.} + h_{hub} \right\}^{T}$.

The translational and rotational hub velocities are subsequently expressed in terms of the *disc* axis set. This is achieved by rotation through the shaft tilt angle, $\gamma_{sh.}$:

$$\underline{v}_{hub}^{disc} = \left[T^{body/disc} \right] \underline{v}_{hub}^{body},$$

$$\underline{\omega}^{disc} = \left[T^{body/disc} \right] \underline{\omega}^{body},$$

where the transformation matrix from body to disc axes is given as:

$$\left[T^{body/disc} \right] = \begin{bmatrix} \cos\gamma_{sh.} & 0 & -\sin\gamma_{sh.} \\ 0 & 1 & 0 \\ \sin\gamma_{sh.} & 0 & \cos\gamma_{sh.} \end{bmatrix}.$$

Similarly, further transformations allow determination of the velocity of a blade element referred to local *blade* axes:

$$\underline{v}_{elem.}^{blade} = \underline{v}_{hinge}^{blade} + \underline{\omega}^{blade} \times \underline{r}_{hinge/elem.}^{blade}$$

$$= \left[u_{elem.}^{blade} \quad v_{elem.}^{blade} \quad w_{elem.}^{blade} \right]^{T},$$

where $\underline{\omega}^{blade} = \left\{ p^{blade} \quad q^{blade} \quad r^{blade} \right\}^{T}$,

and $\underline{r}_{hinge/elem.}^{blade} = \left\{ r_{elem.} \quad 0 \quad 0 \right\}^{T}$.

3.3 Blade Forces

The velocity of a blade element derived above can be used to calculate the aerodynamic forces acting upon each element. Lift and drag per unit span are $\bar{l}_{elem.}$ and $\bar{d}_{elem.}$ respectively. To calculate these forces it is first necessary to determine the tangential and perpendicular components of the velocity of the air over the blade. For a clockwise rotating rotor, Figure 5, the tangential component of velocity of an element is given by:

$$v_{tan.} = v_{elem.}^{blade},$$

and the perpendicular component by:

$$v_{perp.} = w_{elem.}^{blade} - v_{ind.} \cos\beta$$

where $v_{ind.}$ is the induced velocity. Calculation of the elemental lift and drag requires knowledge of the local lift and drag coefficients. These can be found using aerodynamic look-up tables as functions of local Mach number, M and angle of attack, α. The local Mach number is determined by the ratio of the aerodynamic velocity, $v_{aero.}$ - defined as the resultant of the tangential and perpendicular velocity components - to the local speed of sound of air, a:

$$M = \frac{\sqrt{\left(v_{tan.}^2 + v_{perp.}^2 \right)}}{a}.$$

The angle of attack (which, through the inflow model implicitly considers induced effects) is the sum of the incidence of the elemental centre with respect to the airflow, ϕ, and the blade pitch angle, θ:

$$\alpha = \theta + \phi$$

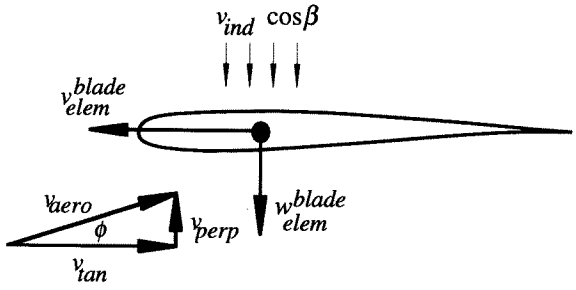

Figure 5: Velocity Components of a Blade Element

The incidence is defined as that relating the tangential and perpendicular velocities:

$$\phi = \tan^{-1}\left(\frac{v_{perp.}}{v_{tan.}} \right),$$

and the blade pitch angle is expressed as a function of blade azimuth position, ψ, and elemental position from the hinge, $r_{elem.}$ as:

$$\theta(\psi, r_{elem.}) = \theta_0 + \theta_{1_s} \sin\psi + \theta_{1_c} \cos\psi + \theta_{twist}(r_{elem.}),$$

where θ_{twist} is the geometric twist of the blade.

Thus linear interpolation of the aerodynamic look-up tables yields estimates of the lift and drag coefficients for each element and the associated forces per unit span can be calculated using expressions in the traditional aerodynamic form:

$$\bar{l}_{elem.} = \frac{1}{2} \rho v_{aero.}^2 c_{elem.} C_l(\alpha, M),$$

$$\bar{d}_{elem.} = \frac{1}{2} \rho v_{aero.}^2 c_{elem.} C_d(\alpha, M),$$

where ρ and $c_{elem.}$ are the air density and the blade element chord respectively.

Knowing the elemental masses and accelerations the inertial forces can also be found. The elemental aerodynamic and inertial forces are added for each element,

transformed via the local inflow angle to the blade axis set and integrated numerically over the span. This gives the shear forces acting at each hinge. Transformations from the blade through to the body axes yields the rotor's contribution to the external forces and moments at the helicopter centre of gravity.

3.3 Blade Flapping Equation

Each blade is assumed to flap about its hinge as a result of the aerodynamic moment, $M_{aero.}$ due to the offset aerodynamic forces acting upon each element. Equilibrium is maintained by the similarly offset inertial elemental forces and a restoring hinge spring producing a moment proportional to the instantaneous flapping angle, β. The second order equation governing blade flapping dynamics about the hinge has been derived from first principles and is expressed as:

$$\ddot{\beta} = -p^{shaft} r^{shaft} \beta^2 + \left(p^{shaft\,2} - r^{shaft\,2} + \frac{M_\beta}{I_\beta} a^{shaft}_{x\,hinge} + \frac{K_\beta}{I_\beta} \right) \beta + \left(p^{shaft} r^{shaft} - \alpha^{shaft}_{y} + \frac{M_\beta}{I_\beta} a^{shaft}_{z\,hinge} \right) + \frac{M_{aero.}}{I_\beta},$$

where K_β is the spring stiffness, I_β is the blade flapping inertia, and M_β is the blade mass moment. The vertical acceleration of the hinge referred to the rotating in-rotor plane shaft axis is represented by $a^{shaft}_{z\,hinge}$. The other terms use similar notation where α indicates rotational acceleration and p, q and r denote components of the angular velocity.

So far in this paper the development of an individual blade rotorcraft model and an inverse simulation methodology capable of accommodating it have been presented. In the following section sample results from this combination are given which show both the validity of the model, and the improved results over the more basic disc model implementation.

4. Inverse Simulations Using an Individual Blade Rotorcraft Model

In this section sample results from the use of the Genisa/Hibrom inverse simulation are compared with results from The Genisa/HGS simulation. The process of validating a mathematical model is essential before there can be confidence in the use of the simulation in practical applications. The results in the following section are therefore aimed at validating the Hibrom model.

4.1 Validation of Hibrom

The most common way of validating a mathematical model is to compare flight test results with those from the simulation. In simple terms a standard control input may be applied to both vehicle and simulation, and the responses of both compared. In the context of an inverse simulation it is possible to fly the vehicle and simulation through identical manoeuvres, then compare both state and control time histories[8].

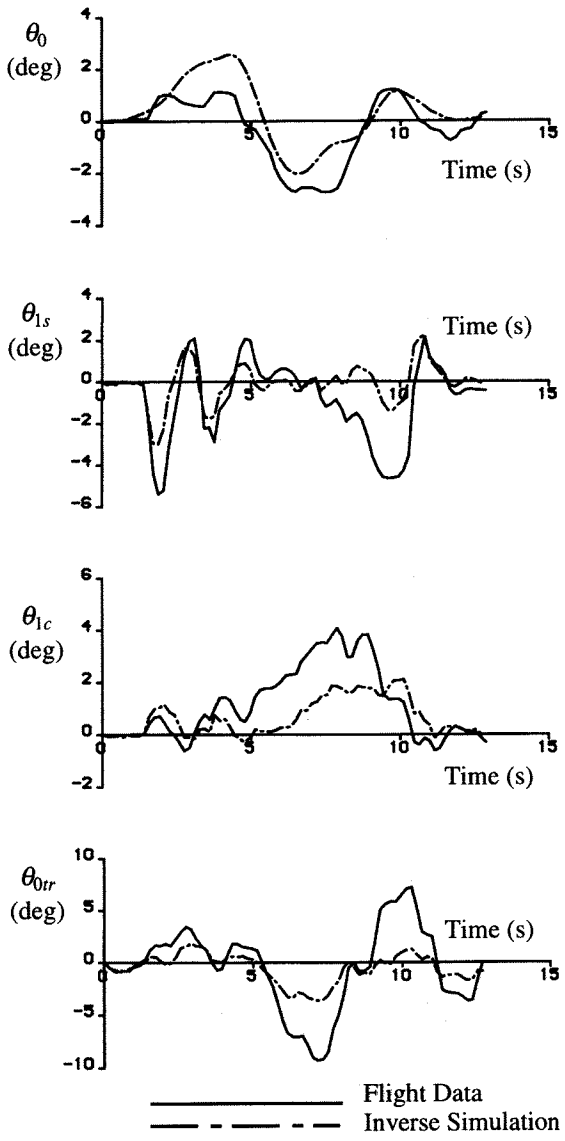

Figure 6: Comparison of Flight Test and Inverse Simulation Results for a Lynx Helicopter Flying a Quick-hop Manoeuvre

For the current study, data from flight trials undertaken by the Defence Research Agency (DRA), Bedford, U.K., has been used. These trials were performed using a Westland Lynx helicopter, and the manoeuvre flown was the "quick-hop". This manoeuvre is initiated from the hover, the pilot being instructed to translate forward to a new location some fixed distance away. Constant altitude and heading is to be maintained, and the aircraft is to be returned to the hover at the final position.

On-board rate gyros and accelerometers permit the vehicle's states to be established throughout the manoeuvre. The pilot's control inputs are also measured allowing blade pitch angles to be obtained. The aircraft's position during the manoeuvre is recorded from ground based measurements.

The flexibility of the integration inverse simulation technique is of particular value when validating mathematical models. It is possible to use the data measured during the trials as the error function for the simulation, in this case we have:

$$\underline{y}_{desired} = \left[\dot{\theta} \quad \dot{\phi} \quad \dot{\psi} \quad \ddot{z}_e\right]^T$$

and with appropriate configurational data in the model it is possible to simulate the Lynx flying precisely that manoeuvre flown by the real aircraft.

Such a comparison is shown in Figure 6 where the measured data from a quick-hop of distance 300ft (91m) has been used. From these plots it is apparent that the overall trends in each case has been captured by the simulation although the amplitude of some inputs do appear to be inaccurate (the initial pulse in longitudinal cyclic, for example). When considering where the modelling deficiencies lie one must consider again the initial assumptions made in constructing the main rotor model. For example, the assumption that the blades are rigid may have a significant effect on the results. The torsional flexibility of the blade will superimpose pitch inputs in addition to those applied by the pilot, an effect which is not present in the mathematical model. Likewise the modelled flapping dynamics and inflow may not completely replicate those of the real aircraft. A disc model is used for the tail rotor, and under-prediction of the collective, θ_{0tr} is consistent with the observations of other authors[18].

The simulation results shown in Figure 6 are sufficiently close to those from the flight tests to give confidence in the model's use in many flight mechanics applications. The type of modelling enhancements required to improve the predictions will require little or no change to the inverse algorithm itself.

4.2 Comparison of Inverse Simulations Using Disc and Individual Blade Rotor Models

A comparison between inverse simulation results from the disc and individual blade models is of obvious interest. One of the first issues to be decided upon is the choice of discretisation interval, Δt. In using a disc model such as HGS in inverse simulation, the choice of discretisation interval is determined primarily by numerical stability. For inverse simulation using an individual blade rotor model further consideration of the solution interval is required. This is due to the influence of the rotor dynamics. Too short a solution interval will result in poor prediction of the influence of control perturbations on the longer term dynamics of the aircraft due to transient effects. This can subsequently lead to failure of the algorithm. Consequently an interval must be chosen which is sufficiently long to allow the transient dynamics to settle. Typically this requires a time consistent with at least half a turn of the main rotor.

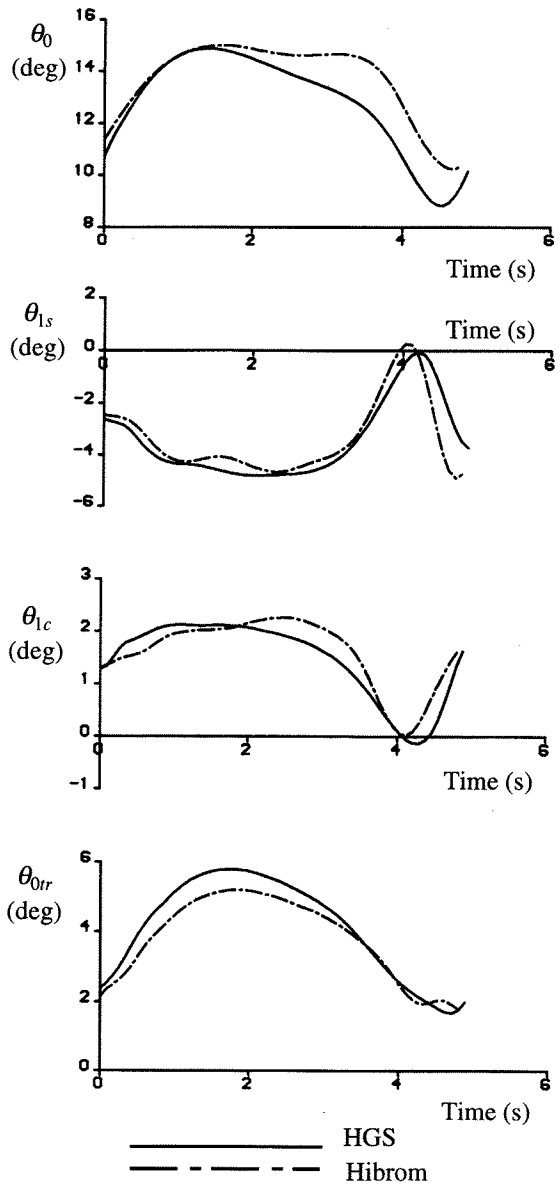

Figure 7 : Inverse Simulation of a Pop-up Manoeuvre (s = 200m, h=25m, V_f = 80kts) with Data for Westland Lynx Helicopter

The oscillatory nature of the rotor forcing also means that the solution interval must coincide with an integer number of main rotor periods (a quarter turn for the 4 bladed helicopter model used here). Note that this effect imposes the constraint of assuming constant rotorspeed on the model. For consistency the same interval (0.086s for the Lynx configuration) is used in both simulations.

A comparison of simulations is shown in Figure 7 for a pop-up manoeuvre. The comparison shows that both models predict very similar control displacements. This may seem like a disappointing result, however it should be borne in mind that this is only a moderately severe manoeuvre and the linear assumptions made in the disc model will be valid. The similarity of the HGS results to the supposedly more realistic individual blade model suggests that disc models are valid for inverse simulation of moderately severe manoeuvres.

4.3 Increased Severity of Manoeuvre

Increasing the severity of the pop-up manoeuvre described in the previous section has a significant effect on the results. Figure 8 shows a comparison of results for the identical pop-up but with the velocity increased to 85 knots. Whilst HGS predicts control displacements which are very similar to those in Figure 7, Hibrom's results are quite different. This is most evident in the discontinuous section of the lateral cyclic time history.

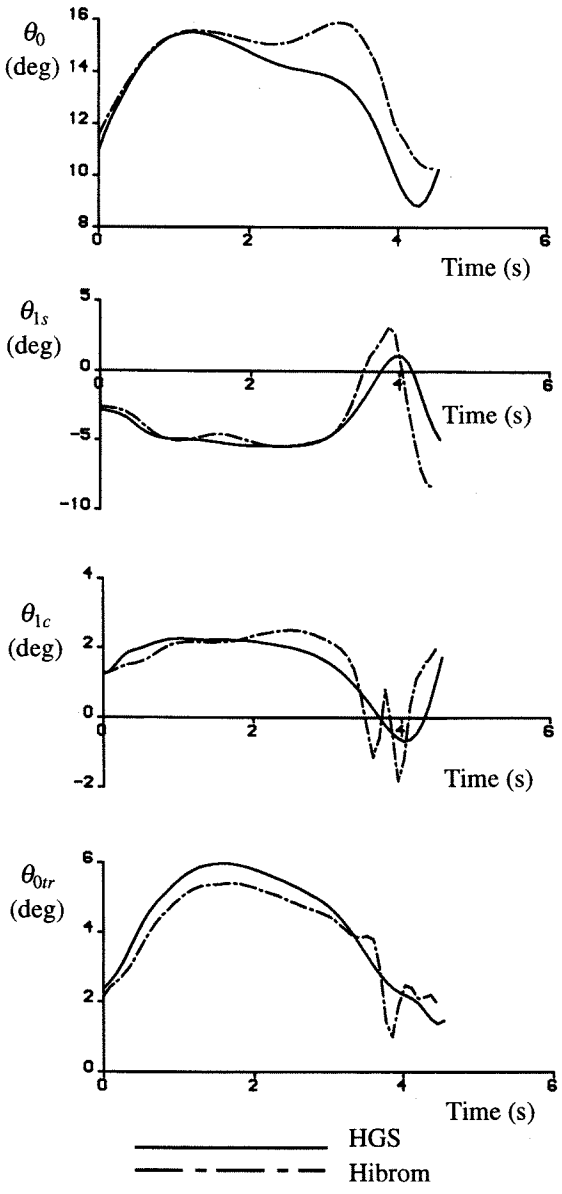

Figure 8 : Inverse Simulation of a Pop-up Manoeuvre (s = 200m, h=25m, V_f = 85kts) with Data for Westland Lynx Helicopter

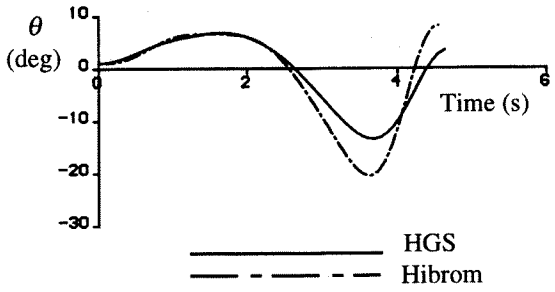

Figure 9 : Fuselage Pitch Angle During Pop-up (85kts) Manoeuvre

This can be explained by consideration of the fuselage pitch angle during the manoeuvre, Figure 9. It can be seen that during the exit phase of the manoeuvre where the aircraft performs a "push-over" (in fact the minimum load factor drops below 0.5g) to clear the obstacle, the fuselage pitch attitude drops to around -20°. At this attitude and flight speed the perpendicular velocity component, $v_{perp.}$, (see Figure 5) becomes negative over a significant portion of the disc. The consequence of this is that on the retreating side of the disc where the tangential velocity, $v_{tan.}$, is small we find large negative angles of attack, α. Figure 10 illustrates the variation of angle of attack of an in-board blade element ($r / R = 0.25$) during the pop-up manoeuvre as predicted by Hibrom. In both simulations the modelled aerofoil section is the NACA 0012 profile, however only the tabulated data used in Hibrom captures the stall characteristics of this section ($\alpha_{C_{l\,max.}} = \pm 15°$). It is clear from Figure 10 that the stall is encountered on the retreating side of the disc throughout the push-over phase of the manoeuvre. The result of this is that a net rolling moment is generated, and the remedial action predicted by Hibrom is a rapid input of lateral cyclic stick to counteract this moment. This effect is entirely missed by the HGS disc model as the stalling characteristics are not predicted by the linear representation of lift coefficient.

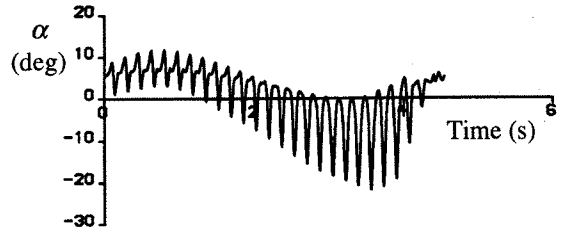

Figure 10 : Angle of Attack of Hibrom Inboard Blade Station During Pop-up (85kts)

It can be argued that such large and rapid inputs are unlikely to be applied by a real pilot. In this case a real pilot would be likely to feel the onset of the stall through vibration, and "ease-off" slightly during the push-over. From the results shown here it is clear that the manoeuvre can be flown well within the control limits of the helicopter, but the low load factor in the push-over phase causes severe blade stalling, an important feature simply not captured by the disc model. In fact as the speed of the helicopter through the manoeuvre is gradually increased (thereby increasing the severity of the manoeuvre) the individual blade model, Hibrom, predicts a limiting case of around 90knots before severe blade stall causes failure of the algorithm (suggesting that this manoeuvre cannot be flown). On the other hand the disc model, HGS, continues to predict solutions well beyond this velocity before control limits are breached. It can be concluded that the linear approximations made in the disc model are insufficient to accurately predict the aerodynamic loading of the rotor in severe flight states. It follows that if accurate results are required for manoeuvres close to the extremities of the flight envelope, then an individual blade rotor model must be used.

5. Conclusions

From the research presented in this paper the following conclusions can be drawn.

i) Helicopter individual blade models require integration methods for inverse simulation in order to accurately predict the wide range of characteristic frequencies.

ii) The discretisation interval should be expressed as a whole number of blade periods to capture the periodicity of the forces. For convenience constant rotorspeed can be assumed to determine the calculation interval.

iii) For improved numerical stability the error function in the inverse algorithm should be based on accelerations rather than displacements.

iv) Valid results are achievable using an individual blade model in inverse simulation. Disc models give equally valid results for most moderate flight conditions.

v) In severe flight conditions disc models do not predict nonlinear aerodynamics effects. In these conditions an individual blade model must be used to guarantee valid results.

As the interest in inverse simulation grows, more effort must be applied to the associated numerical techniques to ensure that the algorithms do not impose constraints on the mathematical models used. If this form of simulation is to be more widely used it must be able to accommodate state-of-the-art mathematical models. The work presented in this paper represents a step forward in achieving this goal.

Acknowledgements

This work is jointly funded by the U.K. Engineering and Physical Sciences Research Council and the Defence Research Agency. The authors wish to thank A. McCallum, M. Charlton and Dr G.D. Padfield of the DRA for their continuing support of this research.

References

1. Thomson, D.G., Talbot, N., Taylor, C., Bradley, R., Ablett, R., "An Investigation of Piloting Strategies for Engine Failures During Take-off From Offshore Platforms", The Aeronautical Journal Vol. 99, No. 981, January 1995.

2. Thomson, D.G., Bradley, R., "Modelling and Classification of Helicopter Combat Manoeuvres", Proceedings of ICAS Congress, Stockholm, Sweden, September 1990.

3. Thomson, D.G., Bradley, R., "The Contribution of Inverse Simulation to the Assessment of Helicopter Handling Qualities", Paper 7.3.2, Proceedings of the 19th ICAS Conference, Anaheim, U.S.A., September 1994.

4. McKillip, R.M., Perri, T.A., "Helicopter Flight Control System Design and Evaluation for NOE Operations Using Controller Inversion Techniques", Proceedings of the 45th Annual Forum of the American Helicopter Society, 1989.

5. Whalley, M.S., "Development and Evaluation of an Inverse Solution Technique for Studying Helicopter Maneuverability and Agility", NASA TM 102889, 1991.

6. Thomson, D.G., Bradley, R., "Development and Verification of an Algorithm for Helicopter Inverse Simulation", Vertica, Vol. 14, No. 2, May 1990.

7. Thomson, D.G., "Development of a Generic Helicopter Mathematical Model for Application to Inverse Simulation", University of Glasgow, Department of Aerospace Engineering, Internal Report No. 9216, June 1992.

8. Bradley, R., Padfield, G.D., Murray-Smith, D.J., Thomson, D.G., "Validation of Helicopter Mathematical Models", Transactions of the Institute of Measurement and Control, Vol.12, No.4, 1990.

9. Rutherford, S., Thomson, D.G., "Development of an Individual Blade Rotorcraft Model for Inverse Simulation of Severe Manoeuvring Flight", University of Glasgow, Department of Aerospace Engineering, Internal Report, In preparation, 1996.

10. Rutherford, S., Thomson, D.G., "Improved Methodology for Inverse Simulation", The Aeronautical Journal, Vol. 100 No. 993 March 1996.

11. Lin, K.C., Lu, P., Smith, M., "The Numerical Errors in Inverse Simulation", AIAA-93-3588-CP, 1993.

12. Gao, C., Hess, R.A., "Inverse Simulation of Large-Amplitude Aircraft Maneuvers", Journal of Guidance, Control, and Dynamics, Vol. 16, No. 4, 1993.

13. Cheney, W., Kincaid, D., "Numerical Mathematics and Computing. Second Edition", Brooks/Cole Publishing, 1985.

14. Prouty, R., "Helicopter Performance, Stability and Control", Krieger, 1990.

15. Turnour, S. R., Celi, R., "Modelling of Flexible Rotor Blades for Helicopter Flight Dynamics Applications", Journal of the American Helicopter Society, January 1996, pp 52-66.

16. Mansur, M.H., "Development and Validation of a Blade Element Mathematical Model for the AH-64A Apache Helicopter", NASA-TM-108863, April 1995.

17. Peters, D.A., HaQuang, N., "Dynamic Inflow for Practical Applications", Journal of the American Helicopter Society, Technical Note, October 1988, pp 64-68.

18. Padfield, G. D., Du Val, R. W., "Application Areas for Rotorcraft System Identification : Simulation Model Validation", AGARD-LS-178, Reference 12, October 1991.